Flux-Flow Resistivity Anisotropy in the Instability Regime of the *a-b* Plane of Epitaxial Superconducting $YBa_2Cu_3O_{7-\delta}$ Thin Films

B. Kalisky,[1,2] P. Aronov,[3] G. Koren,[3,*] A. Shaulov,[1] Y. Yeshurun,[1] and R. P. Huebener[4]

[1]*Department of Physics, Institute of Superconductivity, Bar-Ilan University, Ramat-Gan 52900, Israel*
[2]*Department of Condensed Matter Physics, Weizmann Institute of Science, Rehovot 76100, Israel*
[3]*Department of Physics, Technion-Israel Institute of Technology, Haifa 32000, Israel*
[4]*Institute of Physics, University of Tuebingen, Morgenstelle 14, D-72076 Tuebingen, Germany*

(Received 15 February 2006; published 8 August 2006)

Measurements of the nonlinear flux-flow resistivity ρ and the critical vortex velocity v_φ^* at high voltage bias close to the instability regime predicted by Larkin and Ovchinnikov (Z. Eksp. Teor. Fiz **68**, 1915 (1975) [Sov. Phys. JETP **41**, 960 (1976)]) are reported along the node and antinode directions of the *d*-wave order parameter in the *a-b* plane of epitaxial $YBa_2Cu_3O_{7-\delta}$ films. In this pinning-free regime, ρ and v_φ^* are found to be anisotropic with values in the node direction larger on average by 10% than in the antinode direction. The anisotropy of ρ is almost independent of temperature and field. We attribute the observed results to the anisotropic quasiparticle distribution on the Fermi surface of $YBa_2Cu_3O_{7-\delta}$.

DOI: 10.1103/PhysRevLett.97.067003 PACS numbers: 74.25.Fy, 74.25.Qt, 74.72.Bk, 74.78.Bz

Flux flow due to the Lorentz force in a current carrying type-II superconductor in the mixed state has been studied intensively for many years [1,2]. In view of the $d_{x^2-y^2}$-wave symmetry of the pair wave function in the hole-doped cuprates [3], measurements of the flux-flow resistance (FFR) as a function of the crystallographic direction within the CuO_2 planes become highly interesting. In *c*-axis oriented epitaxial $YBa_2Cu_3O_{7-\delta}$ (YBCO) films under an applied magnetic field parallel to the *c* axis, one could envision an anisotropic behavior resulting in some difference between the flux motion in the node and antinode directions. However, up to now no such anisotropy has been reported, nor has such an effect been analyzed theoretically. Recently, a search study for flux-flow resistivity anisotropy in the low bias pinning regime was carried out by some of us in epitaxial thin films of YBCO [4]. To within the experimental error in that study, no anisotropy was found between the transport properties of microbridges patterned along the node and antinode directions. Since at low bias the transport results are determined by the pinning properties of the films, it was concluded that the pinning properties in YBCO are isotropic. At high bias, however, close to the Larkin-Ovchinnikov (LO) instability regime [5], pinning is negligible and flux-flow resistivity measurements could reveal an intrinsic anisotropy between the node and antinode directions. In this study we present the first experimental results indicating such anisotropy in the *a-b* plane of YBCO films, where the nonlinear FFR along the node direction is enhanced on average by about 10% as compared to that along the antinode direction.

Our measurements were performed on the same two wafers used previously in the low bias measurements [4]. We used two high quality epitaxial, *c*-axis oriented YBCO films of 0.12 μm thickness prepared under identical conditions by laser ablation deposition on (100) $SrTiO_3$ (STO) wafers of 10×10 mm^2 area. The films were patterned with a photolithographic mask into 10 equally spaced $0.12 \times 12 \times 100$ μm^3 bridges along the line dividing the wafer into two halves by deep UV photolithography and Ar ion milling. The dimensions of the resulting bridges were measured with optical and atomic force microscopes and found to conform with the mask design to within $\pm 0.4\%$. Successive microbridges were oriented at alternating angles of 0° and 45° to the edge of the wafers as shown schematically in the upper panel of Fig. 1, so that the transport current would flow either along the node or the antinode directions of the order parameter. The alternating direction of adjacent bridges is important in order to minimize systematic differences due to possible large-scale inhomogeneities in the films. On one film, where the

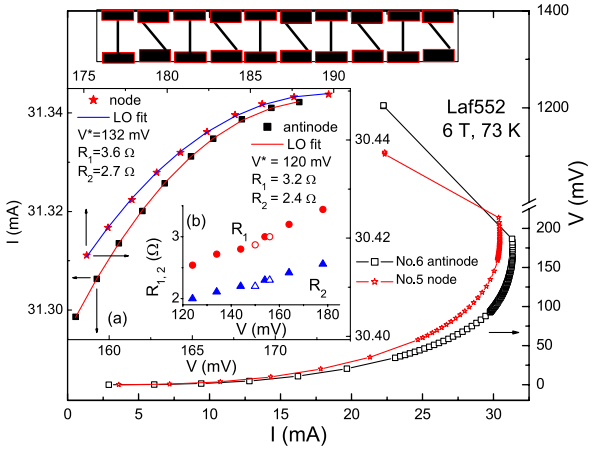

FIG. 1 (color online). A schematic drawing of the bridges on the wafers, and a node and antinode bridges voltage V versus current I at $B = 6$ T and $T = 73$ K. Inset (a) shows the corresponding I versus V just below the maximum of I versus V with fits using Eq. (1), and inset (b) shows the dynamic nature of R_1 and R_2 (see text).

orientation of the STO substrate was with the edge of the wafer parallel to the (010) crystalline direction, five odd number bridges were along the antinode direction, and five even number bridges along the node direction. In the other film where the side of the wafer was parallel to the (110) orientation, the role of the antinode and node bridges was reversed due to the epitaxial growth of the film. Studying these two types of wafers was done in order to check if our ion milling process, done at an incident angle of 45° to the wafers, is affecting the properties of the bridges. Any observed difference in the transport properties of the two wafers would imply that the effect is not intrinsic and results from the patterning process. Low resistance gold contacts were used, and the wafers were annealed for optimal oxygen doping of the films. The resistance measurements were done by the standard four-point dc technique in a helium gas environment with and without a magnetic field of up to 8 T normal to the wafers.

The low bias normal-state resistivity ρ under zero magnetic field was measured versus temperature for each bridge on the two wafers. Averaged values of the innermost bridges are given in Figs. 1 and 2 of Ref. [4]. The onset of the superconductive transition at $B = 0$ was identical for the two kinds of bridges on the two wafers, with $T_c^{\text{onset}} = 94$ K. This value of T_c^{onset} has also been reported by Gross *et al.* [6] for the same kind of films. The resistivity in the normal state at 95 K was $\rho(95\ \text{K}) = 168\ \mu\Omega\,\text{cm}$, being identical for both wafers and both type of bridges. The observation that $\rho(\text{node}) = \rho(\text{antinode})$ results from the fourfold symmetry and the heavy twinning of our films.

At lower temperatures, the FFR in the pinning regime of YBCO was recently found to be isotropic [4]. To determine the pinning-independent FFR we measured the current-voltage characteristic near the LO instability caused by the nonequilibrium distribution of the quasiparticles at moderate electric fields [5]. This instability has been studied in detail in both conventional superconductors and the cuprates [1]. Following procedures of earlier experiments [7], for each temperature and magnetic field, the voltage applied to the sample was ramped up until a resistive jump due to the LO instability was reached. A typical such jump is seen in the I-V curves of Fig. 1. Above this jump a thermal runaway is observed (not shown here), where the bridges reach the normal state with a typical resistivity of 200 $\mu\Omega\,\text{cm}$, which corresponds to about $\rho(105\ \text{K})$. We normally did not expose our bridges to this regime to avoid possible thermal damage. Equation (53) of the LO theory [5] yields

$$I = \frac{V}{R_1}\left\{1 + c\sqrt{1 - \frac{T}{T_c}}\right\} - \frac{V}{R_2}\left(\frac{V}{V^*}\right)^2\left\{1 + \left(\frac{V}{V^*}\right)^2\right\}^{-1}, \quad (1)$$

where c is a number of order unity, V^* is a critical voltage, and R_1 and R_2 are two FFRs which were taken equal in the original theory. We stress that Eq. (1) is valid only in the flux-flow regime at high bias near the maximum of I versus V, and *not* in the pinning regime at low bias. In the low bias regime where I is linear in V, the FFR was found to be isotropic [4], as is expected for a heavily twinned YBCO crystal with a fourfold symmetry if the pinning is also isotropic. By fitting our I-V data in the instability regime using Eq. (1) we find that the FFR $R_1/(1 + \sqrt{1 - T/T_c})$ and R_2 have similar values to within 10%. Since the Lorentz force is oriented perpendicular to the current and the applied magnetic field, and YBCO has a fourfold symmetry, flux flow is along the node direction in the node bridges, and in the antinode direction in the antinode bridges. The resistive voltage across the bridge is $V = |\mathbf{v}_\varphi \times \mathbf{B}|L$, where $\mathbf{v}_\varphi$ is the flux-flow velocity, $\mathbf{B}$ is the magnetic field, and L is the bridge length. The critical voltage V^* in Eq. (1) is thus associated with a critical vortex velocity $\mathbf{v}_\varphi^*$ by this relation.

Joule heating of our samples could affect our results. The possible temperature rise is $\Delta T = \alpha P$, where P is the dissipated electric power per unit area of the sample and α is the thermal boundary resistance [8]. YBCO films on $SrTiO_3$ substrates have $\alpha \cong 10^{-4}\ \text{cm}^2\,\text{K/W}$ at 300 K [8]. Assuming an even larger value of $10^{-3}\ \text{cm}^2\text{K/W}$, and taking the maximum values of P close to the LO instability, we estimate that ΔT remains smaller than a few tenth of a Kelvin. We therefore conclude that Joule heating of our samples can be neglected, except perhaps close to T_c. Experimentally, different rates of the current sweeps (14–300 mA/s) showed reproducibility of the I-V data, thus excluding the possibility of magnetic hysteresis [9] and thermal heating effects.

Two typical I-V curves for a node and antinode bridges are shown in Fig. 1 at $T = 73$ K and $B = 6$ T. The difference between the two curves is very clear and typical of most of our bridges. With increasing current above the critical current regime, the curve becomes steeper and steeper up to the instability. In the case of voltage-controlled operation as we have, a negative differential resistance sets in just before the jump as seen in Fig. 1. In the pinning-independent instability regime, the flux-flow process follows closely Eq. (1). Indeed, in inset (a) of Fig. 1 where ten data points of I versus V just *below* the maximum of I are plotted for each curve, one can see that the fits using Eq. (1) are in excellent agreement with the data. In the fits we assumed that $c = 1$, and obtained R_1, R_2, and V^*. In the following we use the procedure as in inset (a) of Fig. 1 to present our results.

Plots of the flux-flow resistivities $\rho_1/(1 + \sqrt{1 - T/T_c})$ and ρ_2 (calculated from R_1 and R_2) versus the magnetic field B are shown in Figs. 2 and 3 for the two wafers, respectively, at various temperatures. The spread of the midpoint T_c (where the low bias dR/dT is highest) of the different bridges on the two wafers are given in the insets of these two figures. The missing data for bridges No. 4 and No. 9 in Fig. 2 is due to bad contacts. The relatively large spread of the T_c values on this wafer of

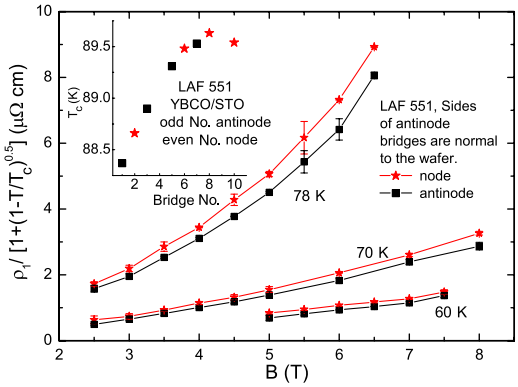

FIG. 2 (color online). Averaged flux-flow resistivity $\rho_1/(1+\sqrt{1-T/T_c})$ versus magnetic field B on LAF551 at 60, 70, and 78 K, for the node (stars) and antinode (squares) directions. The inset shows the distribution of the T_c values on the wafer.

about 1.2 K, and the asymmetry relative to the center of the wafers is due to an off-center alignment of the laser ablated plume on the wafer. Nevertheless, bridges No. 5–8 on LAF551 (Fig. 2) and bridges No. 3–6 on LAF552 (inset of Fig. 3, in a reversed order of the bridges) have a much smaller T_c spread of about 0.4 K. Thus the FFR in these bridges was measured and compared, and no systematic correlation with the corresponding T_c values was found. In Figs. 2 and 3 average values are shown of the two measured node bridges and the two measured antinode bridges on each wafer. The errors in these figures are due mainly to this averaging procedure. These figures show that $\rho_1/(1+\sqrt{1-T/T_c})$ and ρ_2 increase almost linearly with B at low temperatures but more than linearly at higher temperatures. In all cases, a clear anisotropy is observed where the $\rho_1/(1+\sqrt{1-T/T_c})$ and ρ_2 values along the node direction are larger than along the antinode direction. The fact that the *linear* term in Eq. (1) $R_1 \propto \rho_1$ was found to be anisotropic seems to contradict the fourfold symmetry of the twinned crystal. We note, however, that R_1 (and also R_2 and V^*) are voltage dependent [see inset (b) of Fig. 1]. The results of this inset were obtained by fitting the antinode I-V data using Eq. (1) near the instability regime at various voltage segments of $V \pm 5$ mV. The segments contained between 6 data points (above the maximum of I and just below the voltage jump) to 17 points at the lowest voltage bias shown. All fits had R^2 of better than 0.999 (solid symbols). Also shown, are results of two inferior fits with 48 and 65 data points (open symbols), and as one can see, the resulting parameters still follow the general behavior. We thus conclude, that R_1 is not a linear term of the FFR, and therefore does not have to obey the symmetry of the heavily twinned crystal.

Figure 4 shows a histogram of the normalized anisotropy $\Delta\rho_2 = \rho_2(\text{node}) - \rho_2(\text{antinode})$ for all the ρ_2 data on the two wafers. In this figure $\triangle\rho_2$ is normalized by the average value $[\rho_2(\text{node}) + \rho_2(\text{antinode})]/2$ at each field and temperature. We first plotted the normalized anisotropy $\Delta\rho_2$ versus field for the six different temperatures, and found that it is basically field independent to within the noise of the measurements. No systematic temperature dependence of the anisotropy was found at 60, 67, and 77 K as can be seen in the histogram of Fig. 4. This apparently is due to noise in these measurements. At 70, 73, and 78 K, however, one can see that the anisotropy values are concentrated in a narrow range of about 11% ± 2%. We thus conclude that the anisotropy is temperature independent in the temperature range of our measurements. We note that the anisotropy is expected to vanish at high temperatures due to increasing thermalization of the quasiparticles. Above 80 K, however, we could not observe the LO instability jump in the I-V curves to observe this effect.

Next, we turn to the critical voltage V^*, which corresponds to the critical vortex velocity v_φ^* according to $V^* = |\mathbf{v}_\varphi^* \times \mathbf{B}|L$. In Fig. 5 we plot average values of the critical vortex velocity v_φ^* of the node (No. 6,8) and antinode (No. 5,7) bridges on LAF551 versus magnetic field. In

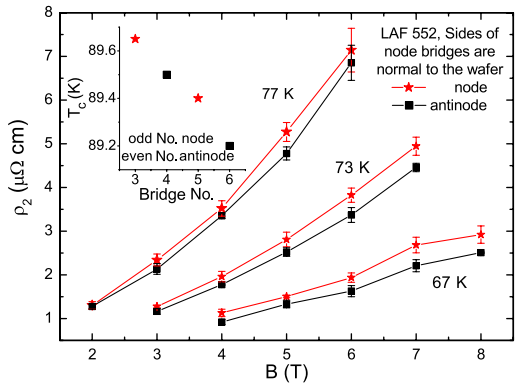

FIG. 3 (color online). Averaged flux-flow resistivity ρ_2 versus magnetic field B on LAF552 at 67, 73, and 77 K, for the node (stars) and antinode (squares) directions. The inset shows the distribution of T_c for the four measured bridges on the wafer.

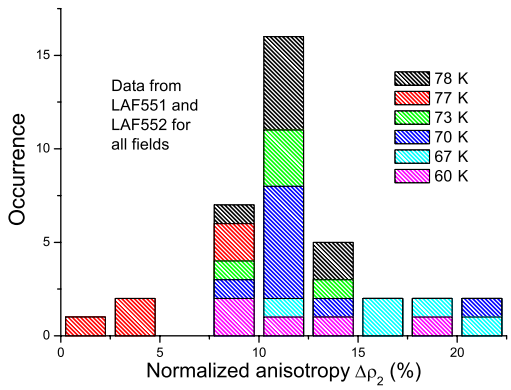

FIG. 4 (color online). Histogram of the anisotropy results on both wafers $\Delta\rho_2 = \rho_2(\text{node}) - \rho_2(\text{antinode})$ normalized by the average value of ρ_2 for all fields and temperatures.

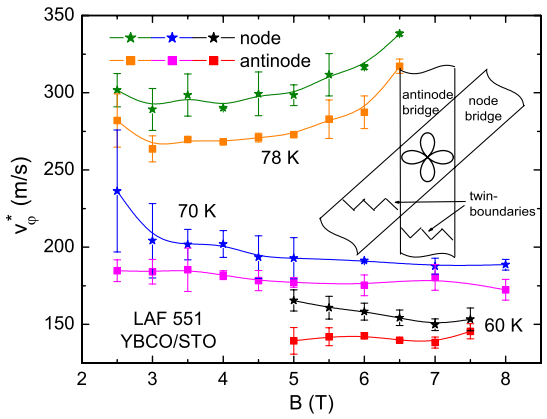

FIG. 5 (color online). Critical vortex velocity v_φ^* calculated from V^* of the fits to Eq. (1) versus B for the node (stars) and antinode (squares) directions for the bridges of Fig. 2. The lines are guide to the eyes. The inset shows a schematic drawing of the twin boundaries in the two kind of bridges.

the node direction v_φ^* is systematically larger (by about 10%–20%) than in the antinode direction. In LAF552 this anisotropy is similar (not shown). The v_φ^* values at each temperature show only a weak field dependence and are basically quite constant as was found previously [7]. Our conclusion therefore is that the anisotropy in v_φ^* is consistent with the anisotropy in ρ_1 and ρ_2, as all have comparable percentage values.

In the absence of a theoretical prediction for the anisotropies of the flux-flow resistivities $\Delta\rho_1$ and $\Delta\rho_2$, and the vortex velocity Δv_φ^*, we shall present simple qualitative arguments for explaining them. In principle, in the absence of pinning, the vortex velocity v_φ^* is affected by the ability of the vortices to transfer momentum to the quasiparticles. The Magnus or Lorentz force that acts on a vortex constantly transfers momentum to it. After a short acceleration, the vortex reaches a terminal velocity v_φ^* in the viscous media while the extra momentum has to be constantly dissipated to the quasiparticle excitations. Thus the easier it is for a vortex to transfer momentum when it moves in a certain direction, the faster it will move in this direction. It was predicted theoretically that in a d-wave superconductor the low energy excitations are located in the vicinity of the nodes [10]. This was verified in photoemission experiments where four small regions of quasiparticle excitations were found on the Fermi surface in the directions of the nodes [11]. Our experimental observations indicate larger flux-flow velocity and FFR in the node direction. Therefore, it seems that the momentum transfer by vortices to the quasiparticles is more effective in the node direction as compared to that along the antinode direction where less quasiparticles are available for the momentum transfer process. Clearly, a comprehensive theoretical analysis of this issue is needed in order to make a detailed quantitative comparison with the present results.

Finally, we rule out the possibility that twinning is responsible for the observed anisotropy. Twins in thin YBCO films form a dense mosaic of elongated crystallites with boundaries along the (110) and (1$\bar{1}$0) node directions as shown schematically in the inset to Fig. 5. If the twin boundaries serve as easy channels for flux flow, then flow in the antinode bridge is unhindered since there is always a Lorentz force component in the direction of the motion. In the node bridge, however, the flow is blocked each time it reaches a boundary normal to its direction. This should lead to a larger flux-flow velocity and FFR in the antinode direction as compared to the node direction. Since this is opposite to the observed results, twins could not be the source of our observations.

In summary, we observed a clear anisotropy in the nonlinear flux-flow resistivities ρ_1 and ρ_2 of YBCO, which we attribute to the intrinsic anisotropy of the low energy quasiparticle distribution on the Fermi surface of a d-wave superconductor. The observed anisotropy in the critical vortex velocity v_φ^* is consistent with the anisotropy of the measured flux-flow resistances.

This research was supported in part by the German-Israel Foundation, the Heinrich Hertz Minerva Center for High Temperature Superconductivity, and the Israel Science Foundation, Grants No. 1565/04 and No. 8003/02. The authors are grateful to A. Auerbach, Th. Dahm, B. Ya. Shapiro, and N. Schopohl for useful discussions.

*Electronic address: gkoren@physics.technion.ac.il

[1] R. P. Huebener, *Magnetic Flux Structures in Superconductors* (Springer, Berlin, 2001), 2nd ed.
[2] M. Tinkham, *Introduction to Superconductivity* (McGraw-Hill, New York, 2001), 2nd ed.
[3] C. C. Tsuei and J. R. Kirtley, Rev. Mod. Phys. **72**, 969 (2000).
[4] G. Koren, P. Aronov, and E. Polturak, Phys. Rev. B **72**, 212503 (2005).
[5] A. I. Larkin and Yu. N. Ovchinnikov, Zh. Eksp. Teor. Fiz. **68**, 1915 (1975) [Sov. Phys. JETP **41**, 960 (1976)].
[6] R. Gross, P. Chaudhari, D. Dimos, A. Gupta, and G. Koren, Phys. Rev. Lett. **64**, 228 (1990).
[7] S. G. Doettinger, R. P. Huebener, R. Gerdemann, A. Kuehle, S. Anders, T. G. Traeuble, and J. C. Villegier, Phys. Rev. Lett. **73**, 1691 (1994).
[8] C. D. Marshall *et al.*, J. Appl. Phys. **73**, 850 (1993).
[9] B. Kalisky, Y. Wolfus, Y. Yeshurun, G. Koren, and R. P. Huebener, Physica (Amsterdam) **401C**, 273 (2004).
[10] G. E. Volovik, Pis'ma Zh. Eksp. Teor. Fiz. **58**, 457 (1993) [JETP Lett. **58**, 469 (1993)].
[11] M. R. Norman *et al.*, Nature (London) **392**, 157 (1998).